Published in final edited form as:
Dev Cell. 2010 December 14; 19(6): 858–871. doi:10.1016/j.devcel.2010.11.005.

Insulin/FOXO Signaling Regulates Ovarian Prostaglandins Critical for Reproduction

Johnathan W. Edmonds[1], **Jeevan K. Prasain**[2], **Dixon Dorand**[1], **Youfeng Yang**[1], **Hieu D. Hoang**[1], **Jack Vibbert**[1], **Homare M. Kubagawa**[1], and **Michael A. Miller**[*]

[1] Department of Cell Biology, University of Alabama at Birmingham, Birmingham, Alabama 35294, USA

[2] Department of Pharmacology and Toxicology, University of Alabama at Birmingham, Birmingham, Alabama 35294, USA

SUMMARY

Abnormalities in insulin/IGF-1 signaling are associated with infertility, but the molecular mechanisms are not well understood. Here we use liquid chromatography with electrospray ionization tandem mass spectrometry to show that the *C. elegans* insulin/FOXO pathway regulates the metabolism of locally acting lipid hormones called prostaglandins. *C. elegans* prostaglandins are synthesized without prostaglandin G/H synthase homologs, the targets of non-steroidal anti-inflammatory drugs. Our results support the model that insulin signaling promotes the conversion of oocyte polyunsaturated fatty acids (PUFAs) into F-series prostaglandins that guide sperm to the fertilization site. Reduction in insulin signaling activates DAF-16/FOXO, which represses the transcription of germline and intestinal genes required to deliver PUFAs to oocytes in lipoprotein complexes. Nutritional and neuroendocrine cues target this mechanism to control prostaglandin metabolism and reproductive output. Prostaglandins may be conserved sperm guidance factors and widespread downstream effectors of insulin actions that influence both reproductive and nonreproductive processes.

Keywords

insulin; FOXO; prostaglandin; *C. elegans*; fertilization; sperm; oocyte; cyclooxygenase; PUFA; lipoprotein

INTRODUCTION

Insulin is an evolutionarily conserved protein hormone that acts downstream of dietary and neuronal signals to integrate metabolic output with reproductive capacity (Burks et al., 2000; Fielenbach and Antebi, 2008; Garofalo, 2002; Ogg et al., 1997; Tissenbaum and Ruvkun, 1998). Its diverse actions include regulation of glucose and fat metabolism, longevity, stress response, and fertility (Mukhopadhyay et al., 2006; Tatar et al., 2003). A canonical signal transduction pathway mediated by the phosphoinositide 3-kinase and serine/threonine kinase

[*]Corresponding author: Michael A. Miller (mamiller@uab.edu).

SUPPLEMENTAL DATA

Supplemental data includes 6 figures, 4 tables, and supplemental experimental procedures.

Akt impinges on the Forkhead Box Class O transcription factor (FOXO) (Landis and Murphy, 2010; Mukhopadhyay et al., 2006). Akt phosphorylates FOXO in the cytoplasm, inhibiting its nuclear translocation. In the nucleus, FOXO can activate or repress transcription of a wide array of genes, often in a tissue-specific manner. In *C. elegans*, insulin deficiency causes low brood size and late progeny production, defects that are suppressed by loss of the FOXO homolog DAF-16 (Gems et al., 1998; Ogg et al., 1997; Tissenbaum and Ruvkun, 1998). Studies in mice have shown that FOXO3a plays a role in ovarian follicle development and ovulation, yet all three FOXO subfamily members are expressed in the mammalian ovary (Castrillon et al., 2003; Liu et al., 2007; Liu et al., 2009; Pisarska et al., 2009). While it is clear that insulin/FOXO signaling plays a critical role in reproduction, the specific processes and molecular mechanisms involved are incompletely understood.

Prostaglandins (PGs) are an important class of lipid hormones called eicosanoids, which are derived from 20-carbon polyunsaturated fatty acids (PUFAs), such as arachidonic (AA) and eicosapentaenoic (EPA) acids (Funk, 2001). PGs are critical for mammalian ovulation, fertilization, implantation, and parturition. The molecular basis for the fertilization defect(s), in particular, is not understood (Gross et al., 1998; Lim et al., 1997; Matsumoto et al., 2001). These labile lipids act close to their synthesis sites, contrasting with systemic protein hormones such as insulin that can act on distant tissues. Mammals lack the desaturase enzymes necessary to convert monounsaturated fatty acids into PUFAs, which must be provided in the diet (Burr and Burr, 1930). The conversion of arachidonic acid to PGH_2 by PG G/H synthase, the target of nonsteroidal anti-inflammatory drugs (NSAIDs) (Vane, 1971), is the rate-limiting step in mammalian PG synthesis (Funk, 2001). PG synthases catalyze the conversion of PGH_2 into biologically active products like PGD_2 and $PGF_{2\alpha}$. PG G/H synthase homologs are not present in nematode, arthropod, and plant genomes (Chandrasekharan and Simmons, 2004). In plants, 18-carbon PUFAs are converted into PG-like jasmonates by a series of enzymes, including allene oxide cyclase (Gfeller et al., 2010).

C. elegans is an attractive model with which to discover the molecular mechanisms regulating reproduction (Han et al., 2010). Its transparent epidermis makes the events of fertilization directly observable in the intact animal (McCarter et al., 1999; Miller et al., 2001). Oocyte maturation and ovulation occur in an assembly line within two gonad arms that are connected to a common uterus. Oocytes in diakinesis of meiotic prophase lie in the proximal gonad next to the spermatheca, the site of sperm storage and fertilization. Sperm crawl across the uterine walls and fertilized eggs to actively target the spermatheca, a process called sperm guidance (Kubagawa et al., 2006). *C. elegans* is the only system available that combines genetic and biochemical manipulation with single cell imaging techniques to study oocyte maturation, ovulation, and sperm guidance *in vivo*.

We have shown that oocye PUFAs are precursors of signals that attract sperm to the spermatheca (Kubagawa et al., 2006). The following model is based on a combination of genetic and biochemical data. PUFAs are synthesized in the intestine and incorporated into yolk lipoprotein complexes. Yolk is secreted into the pseudocoelom and flows to the gonad. The RME-2 low-density lipoprotein receptor mediates yolk endocytosis (Grant and Hirsh, 1999) and PUFA transport to oocytes. Abnormalities in PUFA synthesis or yolk delivery cause nonautonomous sperm motility defects, including reduced velocity and directional velocity, as well as increased reversal frequency (Kubagawa et al., 2006). The chemical identity of the sperm guidance factors is not known, but an RNAi screen identified two glutathione S-transferase enzymes related to mammalian PGD synthases. However, there was no evidence that *C. elegans* synthesizes PGs.

Here we show that the insulin/FOXO endocrine system regulates the synthesis of F-series PGs, which promote sperm motility and reproduction. PG synthesis initiates in the absence of PG G/H synthase homologs. The intestine and germ line are two major sites of DAF-16/FOXO action. DAF-16 represses transcription of genes encoding proteins that deliver PUFAs to oocytes in yolk lipoprotein complexes. Our results support the model that DAF-16 controls a balance in PG metabolism through transcriptional activation and repression mechanisms. In addition to sperm guidance, this balance may influence ovulation, longevity, immunity, and metabolism.

RESULTS

Nonautonomous control of sperm motility by insulin/FOXO signaling

The DAF-2 insulin receptor activates a conserved phosphorylation cascade that inhibits nuclear translocation of the DAF-16/FOXO transcription factor (Fig. 1A). To investigate the basis of the *daf-2* mutant reproductive defects, we examined *daf-2(e1370*) and *daf-2(e1391)* hermaphrodites shifted to the restrictive temperature (25°C) during the L4 and adult stages. The mutants contain functional gametes capable of fertilization, although their oogenesis and oocyte maturation rates are slow (Supplemental Fig. S1). The *daf-2* mutant gonads resemble those from starved hermaphrodites, which have impaired ability to attract motile sperm to the spermatheca (Kubagawa et al., 2006). To test whether *daf-2* is required for sperm targeting, we mated wild-type Mitotracker-labelled (MT) males to adult *daf-2(e1370)* hermaphrodites grown at 25°C for 20–24 hours. Compared to the control, wild-type sperm fail to accumulate efficiently at the spermatheca in *daf-2* mutants 1 hour after mating (Fig. 1B and 2A, B; $P < 0.001$). Similar results are observed in *daf-2(e1391)* mutants (data not shown). *daf-2* mutants grown at the permissive temperature (16°C) do not have sperm targeting defects. The phosphoinositide 3-kinase catalytic subunit *age-1* and serine/threonine Akt/PKB kinase *akt-1* act downstream of *daf*-2 to regulate DAF-16 activity (Fig. 1A) (Landis and Murphy, 2010;Mukhopadhyay et al., 2006). *age-1* and *akt-1* mutants have sperm guidance defects that are similar to *daf-2* mutants (Fig. 1B). *sgk-1* encodes a mammalian serum- and glucocorticoid-inducible kinase ortholog that regulates longevity and oxidative stress, but not dauer and immunity (Fig. 1A) (Evans et al., 2008;Hertweck et al., 2004). Sperm guidance defects are not observed in *sgk-1* mutants (Fig. 1B). We conclude that canonical insulin signaling independent of *sgk-1* is required nonautonomously for sperm guidance in adult animals.

The failure of wild-type sperm to target the spermatheca in *daf-2* mutants is similar to the phenotype of PUFA-deficient hermaphrodites with mutations in *fat* genes. PUFA depletion causes wild-type sperm to migrate with reduced velocity, reduced directional velocity, and increased reversal frequency (Kubagawa et al., 2006). To evaluate sperm motility in *daf-2* mutants, we measured migration values immediately following mating. Compared to the control, wild-type sperm in *daf-2(e1370)* mutant adults shifted to the restrictive temperature for 24 hours migrate with reduced velocity, reduced directional velocity, and increased reversal frequency (Fig. 2F; $P < 0.001$). Therefore, insulin signaling deficiency causes identical sperm migration defects as PUFA deficiency.

Null mutations in *daf-16* partially suppress the *daf-2(e1370)* hermaphrodite brood size defect (Gems et al., 1998; Tissenbaum and Ruvkun, 1998). Similarly, sperm guidance improved significantly in *daf-2(e1370); daf-16(mu86)* double mutants compared to *daf-2(e1370)* mutants (Fig. 2B, F; $P < 0.001$), indicating that sperm motility is inhibited in *daf-2* mutants by increased DAF-16 activity. DAF-16 is required for optimal sperm guidance because *daf-16(mu86)* null mutants have slightly reduced brood size and mild sperm motility defects (Fig. 2C, F; $P < 0.001$). This result suggests that the basal level of DAF-16 present in cell nuclei of wild-type adults is necessary for sperm guidance. Three

lines of evidence support the idea that DAF-16 acts at least partially in the germ line. First, overexpressing DAF-16B in the germ line of wild-type hermaphrodites using the *pie-1* promoter causes sperm guidance defects (Figs. 1B and 2B; $P < 0.001$). Second, *daf-16* RNAi targeted specifically to the germ line using *rrf-1(pk1417)* mutants causes identical sperm guidance defects as *daf-16* RNAi targeted ubiquitously (Fig. 2C). Finally, DAF-16 has been shown to regulate the transcription of germline-specific genes (Curran et al., 2009). We conclude that germline DAF-16 activity is critical for regulating sperm guidance.

Prostaglandins are implicated in sperm guidance

The nonautonomous sperm guidance defects of insulin signaling mutants suggest that DAF-16 regulates the synthesis of sperm guidance factors. Consistent with this hypothesis, DAF-16 transcriptional targets include numerous genes implicated in PUFA metabolism and transport to oocytes, as well as eicosanoid synthesis and breakdown (Supplemental Table S1) (Halaschek-Wiener et al., 2005; Murphy et al., 2003). A previous sperm guidance RNAi screen implicated two genes with similarity to PG synthases (Kubagawa et al., 2006). RNAi depletion of GST-4 or GST-1, which are 34% and 28% identical to human glutathione-requiring PGD synthase, respectively, causes nonautonomous sperm guidance defects. To confirm that *gst-4* is required for sperm guidance, we mated wild-type males to *gst-4(ok2358)* null mutant hermaphrodites. Compared to the wild type, sperm move with reduced velocity and directional velocity in *gst-4(ok2358)* mutants (Figs. 2F; $P < 0.001$), causing reduced spermathecal accumulation (Figs. 2D and 3; $P < 0.001$). Similar results are observed in *gst-4(tm3294)* mutants (data not shown). *gst-4* mutants also have spermathecal valve dilation defects that are similar to *daf-2* mutants and *pie-1p::gfp::daf-16b* transgenic strains (Supplemental Fig. S1). *gst-1* RNAi (Figs. 2D and 3A) did not enhance the sperm guidance defect of *gst-4(ok2358)* null mutants (Fig. 2D), suggesting that GST-1 and GST-4 form a heterodimer or act in sequence. We also identified a predicted PGE synthase called *R11A8.5* and two predicted PGF synthases called *Y39G8B.2* and *C35D10.6* (data not shown) that are required nonautonomously for sperm guidance (Fig. 3). Therefore, multiple predicted PG synthases promote sperm targeting to the spermatheca.

C. elegans synthesizes a wide array of F-series prostaglandins

To determine whether *C. elegans* produces PGs and other eicosanoids, we developed a sensitive liquid chromatography with electrospray ionization tandem mass spectrometry (LC-MS/MS) assay using a liquid/liquid extraction method (see Methods and Supplemental Table S2) (Golovko and Murphy, 2008; Kingsley et al., 2005; Masoodi and Nicolaou, 2006; Murphy et al., 2005). The total ion chromatogram (TIC) obtained from full scan (Q1 scan) LC-MS analysis of wild-type extracts in a mass range of *m/z* 315–360 (typical range used for eicosanoid detection) shows numerous peaks overlapping with PG standard retention times (Fig. 4A; Supplemental Tables S2 and S3). These peaks contain complex mixtures of individual ions. LC-MS/MS analyses indicate that wild-type extracts contain a wide array of PGs that are mostly F-series (Supplemental Table S3 and Supplemental Fig. S2). We decided to focus on F-series PGs because we could not detect significant quantities of D- and E-series PGs in extracts, *gst-4* is required to synthesize specific $PGF_{2\alpha}$ analogs, and authentic $PGF_{2\alpha}$ has potent activity (see below). LC-MS/MS operated in multiple reaction monitoring (MRM) mode with mass transition *m/z* 353/193, which is characteristic of $PGF_{2\alpha}$ and its isomers, detects several $PGF_{2\alpha}$-like compounds (Fig. 4B). The major peak (CePGF2) has a retention time that is almost identical to $PGF_{2\alpha}$. Fragmentation of CePGF2 compared to $PGF_{2\alpha}$ reveals important shared structural features (Fig. 4C, D). The product ion *m/z* 273 results from an initial loss of 44 Da (- C_2H_4O) from the parent ion (*m/z* 353) followed by two 18 Da (-2× H_2O) losses, a pattern indicative of an F-series cyclopentane ring (Fig. 4C, D) (Murphy et al., 2005). This structure is further supported by the presence of an ion at *m/z* 193 that is proposed to result from methyl terminus side chain loss and carbon-14 bond

cleavage. These results indicate that CePGF2 is a $PGF_{2\alpha}$ isomer. CePGF2 may differ from $PGF_{2\alpha}$ by a change in stereochemistry, position of a double bond, or position of the noncyclopentane hydroxyl group. PG G/H synthase homologs are not present in the genome, but myeloperoxidases, which share structural similarity with the PG G/H synthase peroxidase domain (Daiyasu and Toh, 2000), are present. NSAID treatment and RNAi against each of the thirteen myeloperoxidases have little or no effect on sperm guidance (Supplemental Fig. S3). Although we cannot eliminate a role for myeloperoxidases, these results suggest that *C. elegans* synthesizes a wide array of PGs in absence of PG G/H synthase.

Oocyte prostaglandins require intestinal PUFA biosynthesis and transport

To test whether *C. elegans* PGs require synthesis of endogenous C20 PUFAs, we compared wild-type extracts to *fat-3(wa22)* mutant extracts. FAT-3 is a Δ6 desaturase that is necessary for C20 PUFA synthesis and sperm guidance (Kubagawa et al., 2006; Watts et al., 2003). TICs show that many ions in the *m/z* 315–360 range are reduced in *fat-3(wa22)* mutants (Fig. 4A). MRM using the mass transition *m/z* 353/193 indicates that $PGF_{2\alpha}$-like PGs are among those that are reduced. Therefore, CePGF2 and other PGs require endogenous C20 PUFA synthesis (Fig. 4B). Intestinal PUFAs are transported to oocytes in yolk lipoprotein complexes (Kubagawa et al., 2006). Loss of the RME-2 low-density lipoprotein/yolk receptor, which is specifically expressed in oocytes (Grant and Hirsh, 1999), causes severe sperm guidance defects. TICs show that PG levels are broadly reduced in *rme-2(b1008)* null mutants compared to the wild type (Fig. 4E). MRM using the mass transition *m/z* 353/193 demonstrates that most $PGF_{2\alpha}$-like PGs, including CePGF2, are decreased in *rme-2* mutants (Fig. 4F). *gst-4* is not essential for CePGF2 synthesis (data not shown), but it is essential for synthesis of *rme-2*-dependent unsaturated $PGF_{2\alpha}$ analogs, detected using MRM with mass transition *m/z* 351/271 (indicated by arrow, Fig. 4G). Therefore, GST-4 is required to synthesize certain oocyte F-series prostaglandins. We conclude that production of CePGF2 and other F-series PGs requires endogenous intestinal C20 PUFA synthesis and transport to oocytes.

F-series prostaglandins are sufficient to promote sperm motility *in vivo*

We considered two possibilities to explain the current data. Either sperm express signal transduction machinery that regulates their motility, or lipids alter the uterine environment and indirectly influence motility. Indirect support for the first possibility comes from direct observation. Uterine cells do not contract and fluid flow does not contribute to sperm motility in our guidance assays. To test whether sperm guidance requires signal transduction, we sought to identify machinery that function in sperm. We identified a G protein-coupled receptor (GPCR) of the Srb chemoreceptor family called *srb-13* that is required autonomously in sperm for guidance to the spermatheca (Fig. 3). *srb-13* mRNAs are expressed during spermatogenesis (Reinke et al., 2004) and *srb-13*, *gst-4*, *R11A8.5*, and multiple *fat* genes physically lie within chromosomal regions enriched in genes important for sperm and oocyte communication (Miller et al., 2004). *srb-13* mutant sperm are motile, capable of fertilization, able to induce oocyte maturation and ovulation, and resemble wild-type sperm in morphology. However, the mutant sperm do not target the spermatheca efficiently in wild-type or *daf-16(mu86)* hermaphrodites (Fig. 3A and data not shown). When wild-type sperm are mated to *srb-13* mutant hermaphrodites, sperm guidance defects are not observed (Fig. 3A). Collectively, the data support the hypothesis that sperm guidance requires PG synthesis in oocytes and *srb-13* function in sperm.

Next, we developed an *in vivo* assay to measure sperm migration velocity in *fat-2(wa17)* and *rme-2(b1008)* PUFA-deficient mutants following lipid addition (Fig. 5A, B). In this assay, sperm pseudopod translocation rate across eggs and uterine walls is measured within

minutes of lipid microinjection (Supplemental Fig. S4). Microinjecting 1/20 and 1/200 dilutions of wild-type extracts into the uteri of PUFA-deficient mutants causes a robust sperm velocity increase (Fig. 5C; $P < 0.001$). Wild-type extracts have more activity than *rme-2* mutant extracts, consistent with their increased PG levels (Fig. 5C; $P<0.005$). The assay was then used to assess the bioactivity of diverse human eicosanoids. Microinjecting 25μM concentrations of $PGF_{2\alpha}$, PGD_2, or PGE_2 stimulates sperm velocity as well as wild-type extracts (Fig. 5B-D). These PGs have similar structures consisting of a saturated cyclopentane ring with at least one hydroxyl group (Fig. 5B). PGI_2 and carbaprostacyclin, a stable PGI_2 analog, have moderate activity, whereas Thromboxane B_2, Leukotriene B_4, and Lipoxin A_4 have no activity (Fig. 5D). These results indicate that sperm recognize the PG cyclopentane ring and respond with a velocity increase (Fig. 5B, D). The mechanism by which PGs stimulate sperm motility is increased pseudopod translocation (Supplemental Fig. S4).

PGs function in high picomolar to nanomolar concentrations *in vivo*. We titrated down the microinjected concentrations, which represent an upper limit because of dilution and loss through the vulva. Microinjecting 250nM and 25nM $PGF_{2\alpha}$ stimulates sperm motility ($P < 0.001$), but 250nM PGD_2 does not (Fig. 5E; $P > 0.05$). $PGF_{3\alpha}$, which is derived from EPA, also has potent activity (Fig. 5E; $P < 0.001$). The response to $PGF_{2\alpha}$ saturates above 250nM, consistent with a receptor-mediated process (Fig. 5E). We conclude that F-series PGs are sufficient to stimulate sperm motility at nM concentrations and that this effect is likely to be a direct response.

Insulin/FOXO signaling regulates prostaglandin synthesis

We hypothesized that insulin signaling promotes oocyte PG synthesis. To test this hypothesis, we compared PG levels in wild-type extracts to *daf-2* mutant extracts. TICs show that *daf-2* mutants have a broad reduction in numerous PGs (Fig. 6A). The DAF-2-dependent mechanism appears to have some specificity for PG-like lipids because more hydrophobic lipids such as hydroxyeicosatetraenoic acids, which have retention times in the 17–20 min range, are not broadly reduced. MRM using the mass transition *m/z* 353/193 demonstrates that CePGF2 is among those PGs that are reduced (Fig. 6B). Our genetic data indicate that *daf-16* inhibits sperm guidance in *daf-2* mutants (Fig. 2B, F). The *daf-2(e1370); daf-16(mu86)* TIC shows a general increase in PG levels compared to the *daf-2(e1370)* TIC (Fig. 6A). However, closer inspection reveals dynamic regulation. MRM indicates that increased DAF-16 activity in *daf-2* mutants causes decreased levels of RME-2-dependent PGs, such as CePGF2 (Fig. 6B). These PGs are important for sperm guidance (Figs. 2–5) and possibly ovulation (Supplemental Fig. S1). We also identified DAF-16-dependent PGs whose levels increase in *daf-2* mutants (Supplemental Fig. S5A). These PGs do not require RME-2 for synthesis (Supplemental Fig. S5A) and may modulate lifespan, immunity, and metabolism (Supplemental Table S4). We conclude that insulin/FOXO signaling regulates synthesis of a wide range of PGs, including sperm-targeting F-series PGs.

FOXO inhibits PUFA delivery to oocytes in lipoprotein complexes

To investigate the mechanism by which DAF-16 inhibits PG synthesis, we examined DAF-16 transcriptional targets (Supplemental Table S1). DAF-16 represses transcription of all six *vit* genes, which encode ApoB-100 homologs that form yolk lipoprotein complexes, and of genes implicated in lipoprotein transport and PG synthesis (Halaschek-Wiener et al., 2005; Murphy et al., 2003). Yolk can be directly observed in hermaphrodites using DIC microscopy and a *vit-2p::vit-2::gfp* transgene, which contains one of two predicted DAF-16 binding sites in the *vit-2* promoter (Grant and Hirsh, 1999; Murphy et al., 2003). We observe a DAF-16-dependent decrease in yolk lipoprotein pools within the pseudocoelom and gonad

of *daf-2(e1370)* mutants (Fig. 6C). Yolk synthesis in the intestine and endocytosis into the oocytes, visualized using the *vit-2p::vit-2::gfp* transgene, decreases in time following shifting of *daf-2(e1370)* mutants to the restrictive temperature (Fig. 6D). Massive yolk accumulation is observed in the pseudocoelom of *pie-1p::gfp::daf-16b* transgenic hermaphrodites, suggesting that germline DAF-16 inhibits yolk endocytosis (Fig. 6C). We confirmed this effect using the *vit-2p::vit-2::gfp* reporter (Fig. 6D). Therefore, DAF-16 acts in the intestine to prevent yolk synthesis and in the germ line to prevent yolk endocytosis. We conducted mass spectrometry analysis to confirm that yolk-derived PGs are reduced in *daf-2* mutants. TICs show that largely overlapping sets of lipids are reduced in *daf-2* and *rme-2* mutants (Supplemental Fig. S5B-D). Additional levels of regulation may also exist, as DAF-16 transcriptional targets include genes involved in PG synthesis and breakdown (Supplemental Table S1). However, *daf*-16 RNAi did not suppress the *gst-4(ok2358)* sperm guidance defect, suggesting that DAF-16 does not influence GST-4 activity in oocytes (data not shown). These results demonstrate that insulin/FOXO signaling regulates oocyte PG synthesis in part by controlling PUFA delivery in lipoprotein complexes.

Transcription repression (directly or indirectly) is the mechanism by which DAF-16 regulates *vit* gene expression in the intestine (Halaschek-Wiener et al., 2005; Murphy et al., 2003). To investigate the mechanism operating in the germ line, we analyzed genome-wide DNA microarray datasets (Fig. 6E) (Murphy et al., 2003; Reinke et al., 2004). Of 263 genes with transcript levels up-regulated by DAF-16, none are expressed in germ cells undergoing oogenesis. In contrast, 14 genes are expressed during oogenesis with transcripts down-regulated by DAF-16. Somatic cells have an equal mix of DAF-16-regulated genes. We conclude that transcriptional repression is likely to be the major mechanism by which DAF-16 inhibits sperm guidance.

Dietary and neuronal control of sperm guidance

Dietary and neuronal cues modulate insulin/FOXO signaling in *C. elegans*, *Drosophila*, and mammals. We hypothesized that these mechanisms might integrate nutritional status and metabolism with reproductive output, in part by regulating sperm guidance. In the *C. elegans* intestine, the FAT-2 Δ12 fatty-acyl desaturase converts dietary monounsaturated fatty acids into PUFAs (Watts and Browse, 2002). *fat-2(wa17)* hermaphrodites have reduced PUFA levels (Watts and Browse, 2002), elevated DAF-16 target gene expression (Horikawa et al., 2008), severe sperm guidance defects (Kubagawa et al., 2006), and decreased CePGF2 levels (Supplemental Fig. S6A). To investigate the mechanism by which PUFAs influence DAF-16 transcriptional activity, we generated *fat-2(wa17); sod-3p::gfp* integrated transgenic mutants. *sod-3* is a direct DAF-16 target (Henderson et al., 2006; Oh et al., 2006). *fat-2* mutants have elevated *daf- 16*-dependent GFP expression throughout the body that is suppressed by PUFA supplementation (Fig. 7A). To examine the effects of PUFAs on yolk dynamics, we generated *fat-2(wa17); vit-2p::vit-2::gfp* mutants. These hermaphrodites generate substantial yolk, but endocytosis into oocytes is severely compromised (Fig. 7B, C). Again, PUFA supplementation rescues the defects. When *fat-2* mutant adults are exposed to *daf-16* RNAi for 24 hours, the sperm guidance defects are partially rescued (Fig. 2E; $P < 0.001$). The data support the model that PUFAs inhibit DAF-16 activity to promote oocyte lipoprotein complex endocytosis and oocyte PG synthesis.

DAF-16 stimulates transcription of seven fatty acid desaturases that mediate PUFA synthesis (Supplemental Table S1) (Halaschek-Wiener et al., 2005; Murphy et al., 2003), suggesting that DAF-16 may be part of a PUFA homeostasis mechanism. We found that *fat-2* mutants synthesize significant quantities of PGs, many of which are not synthesized in the wild type (Supplemental Fig. S6A, B). Therefore, the small amount of Δ12 fatty-acyl desaturase activity in *fat-2(wa17)* mutants is sufficient for PG synthesis. These PGs do not appear to require yolk endocytosis (Fig. 7B, C). *fat-2(wa17); daf-16(mu86)* mutants are sick

in appearance and have severe germline development defects, contrasting with fertile *fat-2(wa17)* mutants (Supplemental Fig. S6C). The double mutants do not expand in population size and cannot be maintained in the absence of PUFA supplementation, which rescues the survival and germline development defects. We conclude that DAF-16 compensates for low PUFA levels during development and inhibits reproduction in adults.

Metabolism, nutritional status, and longevity are regulated by a neuroendocrine system consisting of insulin, serotonin, and TGF-β pathways that converge on DAF-16 (Fielenbach and Antebi, 2008; Ogg et al., 1997; Shaw et al., 2007). Serotonin-deficient *tph-1(mg280)* mutants have elevated DAF-16 activity throughout the body and reduced brood size (Liang et al., 2006; Sze et al., 2000). *tph-1* is expressed specifically in serotonergic neurons. To test whether serotonin deficiency influences sperm guidance, we mated wild-type males to *tph-1(mg280)* hermaphrodites. Relative to the control, sperm in *tph-1(mg280)* hermaphrodites migrate with reduced directional velocity and increased reversal frequency, causing reduced spermathecal accumulation (Figs. 2E, F and 3A; $P < 0.001$). Similarly, mutations in the *daf-4* type II TGF-β receptor (Estevez et al., 1993) and *daf-7* TGF-β ligand (Schackwitz et al., 1996) cause nonautonomous sperm targeting defects (Fig. 3A). *daf-7* is specifically expressed in ASI sensory neurons. Taken together, these data support the model that the neuroendocrine system modulates reproductive capacity, in part through control of PG metabolism critical for sperm guidance.

DISCUSSION

Insulin's actions include the regulation of longevity, stress response, immunity, metabolism, and reproduction (Mukhopadhyay et al., 2006; Tatar et al., 2003). How these responses are specified is not well understood. Here we show that insulin/FOXO signaling modulates the synthesis of locally acting lipid hormones called PGs. Our results, together with those of previous studies, support the following model (Fig. 8). Insulin acts through a canonical pathway to promote oocyte PG synthesis. When insulin levels drop, DAF-16 enters the nucleus and acts alone or in combination with other factors to activate and repress gene transcription in a cell-type specific fashion. DAF-16 inhibits the transport of intestinal PUFAs to oocytes in yolk lipoprotein complexes. This mechanism, and perhaps additional mechanisms, down-regulates oocyte F-series PG synthesis critical for sperm guidance and likely ovulation. In the intestine, DAF-16 stimulates the transcription of genes encoding proteins that increase yolk-independent PG synthesis, which may influence longevity, immunity, and metabolism (Supplemental Table S4). Dietary fat intake, as well as neuronal serotonin and TGF-β pathways inhibit DAF-16 to promote sperm guidance and reproduction.

We show that insulin signaling is required in adults to promote multiple reproductive processes, including oogenesis, oocyte maturation, ovulation, and sperm guidance. Recent studies support the idea that mild reduction in insulin signaling can delay aging-associated changes in oocyte quality (Hughes et al., 2007; Luo et al., 2010). Whether PGs influence oogenesis, oocyte maturation, or reproductive aging is not clear. DAF-16 acts on multiple levels to inhibit oocyte PG synthesis and at least two levels appear to involve transcriptional repression. DAF-16 directly or indirectly represses vitellogenenin gene expression in the intestine (Halaschek-Wiener et al., 2005; Murphy et al., 2003), preventing yolk formation. In the germ line, overexpression of the DAF-16B isoform inhibits oocyte yolk endocytosis. The germline DAF-16 target(s) is not known, but DNA microarray data suggest the target is transcriptionally repressed (Murphy et al., 2003; Reinke et al., 2004). Based on these data, DAF-16 is likely to act in transcriptionally active, developing oocytes and intestinal cells to suppress oocyte PG synthesis.

Three lines of evidence support the hypothesis that F-series PGs guide migrating sperm to the spermatheca. First, oocytes synthesize multiple F-series PG analogs, whose abundances (roughly 20 pM to 2 nM per ion per worm) correlate with a wide range of mutants causing nonautonomous sperm guidance defects. Significant levels of D- and E-series PGs were not found in the extracts. Second, predicted PGD, PGE, and PGF synthases (a.k.a. aldo-keto reductases) are necessary for sperm guidance. In mammals, aldo-keto reductases can act downstream of PGD and PGE synthases to generate F-series PGs (Fig. 8B). Finally, microinjecting nanomolar concentrations of F-series PGs, but not other eicosanoids into PUFA-deficient hermaphrodites stimulate a robust increase in sperm velocity. PG microinjection through the vulva does not influence directional velocity, likely because a continuous gradient is not established. Given that sperm migrate with decreased velocity and directional velocity, as well an increased reversal frequency in PG-deficient mutants, we favor the model that F-series PGs control sperm guidance. The numerous RME-2-dependent $PGF_{2\alpha}$ and $PGF_{3\alpha}$ analogs present in wild-type extracts suggest that multiple structurally distinct F-series PGs derived from differernt precursors promote sperm guidance. This idea is further supported by data indicating that deficiency in either AA or EPA alone does not cause sperm guidance defects, but deficiency in all C20 PUFAs does (Kubagawa et al., 2006). Whether different precursors generate PGs with distinct signaling properties is not known.

PG G/H synthase or cyclooxygenase is a bifunctional enzyme with two distinct active sites that catalyze the cyclization of AA into PGG_2 and the peroxidase-mediated reduction of PGG_2 into PGH_2 (Chandrasekharan and Simmons, 2004) (Fig. 8B). PG G/H synthase homologs are found in cnidarian, tunicate, and vertebrate genomes, but not in nematode and arthropod genomes. The most parsimonious explanation is that PG G/H synthases were lost in nematodes and arthropods. There is considerable evidence that PG synthesis is an evolutionarily conserved feature of multicellular animals (Rowley et al., 2005; Sommer et al., 2003; Stanley-Samuelson and Pedibhotla, 1996; Tootle and Spradling, 2008). However, structural data are lacking in most invertebrates. A recent report suggests that a *Drosophila* myeloperoxidase called Pxt has cyclooxygenase activity, although the mechanism and synthesis products are not clear (Tootle and Spradling, 2008). The myeloperoxidase domain is structurally related to the PG G/H synthase peroxidase domain, but myeloperoxidases do not possess a known cyclooxygenase active site (Daiyasu and Toh, 2000). We show that *C. elegans* synthesizes numerous F-series PGs, including CePGF2. Although complete structures cannot be determined at present, LC-MS/MS data are consistent with several F-series PGs containing the cyclopentane ring at different positions in the carbon backbone (data not shown). We also identified F-series PGs with fewer than 18 carbons, suggesting that the backbone is cleaved. Structural and NSAID results, together with the lack of PG G/H synthases in the genome, support the model that PG synthesis initiates by an alternative mechanism. We could not find evidence for involvement of myeloperoxidases, but cannot eliminate the possibility that they are involved. These results suggest that cyclopentane ring formation is catalyzed by a enzyme other than PG G/H synthase, similar to plant and protozoan species (Dey et al., 2003; Gfeller et al., 2010).

gst-1 and *gst-4* encode predicted PGD synthases and *R11A8.5* encodes a predicted PGE synthase. However, LC-MS/MS data indicate that D- and E-series PGs are either present at low levels or not present in extracts. It is possible that these predicted synthases produce transient D- and E-series intermediates, respectively that are rapidly converted into F-series PGs by aldo-keto reductases (Fig. 8B). Five aldo-keto reductases show germline expression (Reinke et al., 2004) and two tested thus far by RNAi are necessary for sperm guidance. However, an alternative possibility is that GST-1, GST-4, and R11A8.5 generate F-series PGs directly. The biochemical mechanisms for PG synthesis remain to be determined. There is evidence that *gst-1* and *gst-4* are expressed in multiple tissues, including the germ line,

and that expression is regulated by stress and infection (Leiers et al., 2003;Reinke et al., 2004;Shapira et al., 2006;Troemel et al., 2006). The *C. elegans* genome encodes a wide array of predicted PG synthases with complex expression patterns and PG synthesis is likely to occur in numerous cell types.

Whether FOXO regulates prostaglandin metabolism in other animals is not clear. In mammals, FOXO1, FOXO3, and FOXO4 are expressed in overlapping patterns within the ovary (Castrillon et al., 2003; Liu et al., 2007; Pisarska et al., 2009). FOXO3a knockout mice exhibit accelerated follicular development (Castrillon et al., 2003), whereas oocyte-specific FOXO3a activation inhibits follicular development and causes anovulation (Liu et al., 2007). Evidence is accumulating that mammalian oocytes and cumulus cells secrete unidentified sperm chemoattractants, but little is known about the *in vivo* mechanism (Eisenbach and Giojalas, 2006). A recent study has shown that FOXO1 expression in granulosa cells suppresses the transcription of numerous genes involved in fatty acid and steroid metabolism, including the sterol element-binding transcription factors SREBP1 and SREBP2 (Liu et al., 2009). In endothelial cells, SREBPs bind to the COX-2 promoter and induce its expression (Smith et al., 2005). COX-2-dependent prostaglandins are critical for ovulation and fertilization, but not for follicle development (Lim et al., 1997; Matsumoto et al., 2001). It is not known if prostaglandins are involved in sperm guidance, but COX-2 is expressed in cumulus cells of ovulated oocytes (Lim et al., 1997). NSAIDs inhibit ovulation and fertilization in a wide range of mammals and are associated with reversible infertility in human females (Mendonca et al., 2000; Pall et al., 2001; Sirois et al., 2004; Smith et al., 1996). These studies highlight intriguing similarities between *C. elegans* and mammals. However, there are also important differences, particularly in the site(s) of insulin, FOXO, and prostaglandin actions and possibly in the reproductive processes involved. Determining the extent to which similarities between *C. elegans* and mammals are rooted in an ancestral mechanism will require further investigation.

EXPERIMENTAL PROCEDURES

Strains and Sperm Guidance Assays

C. elegans strains were maintained as previously described (Kubagawa et al., 2006). MitoTracker Red CMXRos (Invitrogen) was used to label wild-type or *fog-2(q71)* male sperm (Kubagawa et al., 2006). Briefly, Mitotracker CMXRos solid was diluted to 1mM in DMSO. Approximately 100 males were transferred to a watch glass containing Mitotracker CMXRos diluted to 10 μM in a total volume of 300 μL M9 buffer. The males were incubated in the dark for 2–3 hours, transferred to an NGM plate seeded with *E. coli*, and then transferred again for overnight recovery. For sperm migration assays, 10–20 adult hermaphrodites were anesthetized with 0.1% tricaine and 0.01% tetramisole hydrochloride in M9 buffer for a period of 30 minutes (McCarter et al., 1999). The adults were transferred to an NGM plate containing an ~1 cm circle of bacteria and ~50 Mitotracker-labelled males. Males were allowed to mate for 30 minutes. Most mutants/RNAi hermaphrodites have variable sperm guidance defects. For sperm accumulation experiments, mated hermaphrodites were separated from labelled males for 1 hour before mounting on 2% agarose pads for microscopy. For analysis of sperm motility, hermaphrodites were mounted on agarose pads immediately after mating, as previously described (Kubagawa et al., 2006). Sperm migration was measured from traces generated from time-lapse videos. Both DIC and fluorescent images were taken every 30 seconds. Axiovision software was used to measure distances. See supplemental experimental procedures for strains, RNAi methods, and additional details.

PUFA supplementation

PUFA-containing NGM plates were prepared as previously described (Kubagawa et al., 2006; Watts and Browse, 2002). Briefly, PUFAs were added slowly to cooled NGM media, with stirring, to final concentrations of 100–200 μM. Plates were kept in the dark and seeded with NA22 bacteria after 24 hours. NA22 bacteria accumulate PUFAs into their lipids at ranges from 1–5% (Kubagawa et al., 2006). See supplemental experimental procedures for additional information.

Drug Treatment

For treatment with indomethacin (IC_{50} < 6 μM) and acetylsalicylic acid (aspirin, IC_{50} < 1.25 mM), hermaphrodites were exposed to the drugs on plates and in M9 buffer. For plates, the drugs were mixed with cooled NGM and the pH was adjusted to 7.0. Control plates were prepared using DMSO only (< 2%). For liquid exposure, drugs were diluted in M9 buffer and added to watch glasses containing M9 buffer. The pH was checked and adjusted to ~7.0, if necessary. Adult hermaphrodites were incubated with the drugs for 4–16 hours (plus food if incubations exceeded 8 hrs.). For liquid culture, DMSO was kept below 0.5%. For treatment with the selective COX-1 inhibitor SC-560 (IC_{50} < 1 nM) and the selective COX-2 inhibitor CAY-10404 (IC_{50} = 9 nM), worms were incubated with drugs in M9 buffer for 4–8 hrs. SC-560, CAY-10404, and controls include fresh DMF (≤0.04%). See supplemental experimental procedures for additional information.

Transgenics

The *pie-1p::gfp::daf-16b* transgenic strain was generated using the microparticle bombardment method (Praitis et al., 2001). The *daf-16b* ORF was cloned into the pID3.01B GFP bombardment destination vector using Gateway LR cloning (Invitrogen). See supplemental experimental procedures for additional details.

Microinjection

Lipid extracts and commercial eicosanoids (Cayman Chemical) were microinjected through the vulva into the reproductive tract, as previously described (Kubagawa et al., 2006). *fat-2(wa17)* or *rme-2(b1008)* hermaphrodites were mated with MitoTracker-labeled males before microinjection. Fresh nitrogen-purged lipids were dissolved in ethanol, diluted in M9 buffer, and loaded in the needle. See supplemental experimental procedures for additional details.

Lipid Extraction

A mixed-stage population of each strain was grown on sixty 150mm seeded NGM plates. For comparative analysis, tissue was weighed to ensure that equal amounts were analyzed. Individual samples differed by less than 1% total mass. During and following extraction, extreme care was taken to prevent oxidation. Samples were dried and stored in glass vials (at −20 °C) under nitrogen gas and 0.005% butylated hydroxy-toluene (BHT) was added to solvents. For liquid/liquid extraction, a previously published procedure for extracting PGs from mammalian tissue (Golovko and Murphy, 2008) was adapted for *C. elegans*. See supplemental experimental procedures for additional details.

Mass spectrometry

LC-MS/MS analyses of commercial standards and *C. elegans* extracts were performed using a system consisting of a Shimadzu Prominence HPLC with a refrigerated auto sampler (Shimadzu Scientific Instruments, Inc. Columbia, MD), and an API 4000 (Applied Biosystems/MDS Sciex, Concord, Ontario, Canada) triple quadrupole mass spectrometer. The chromatographic separation was performed on a Synergy hydro RP-C18 column (250 ×

2.0 mm i.d) pre-equilibrated with 0.1% formic acid. The LC-MS/MS system was controlled by BioAnalyst 1.4.2 software. Twenty-seven eicosanoid standards (Cayman Chemical) were used for optimization (Supplemental Table S2). For comparative analysis of different strains, the extracts were run consecutively. See supplemental experimental procedures for additional details.

Supplementary Material

Refer to Web version on PubMed Central for supplementary material.

Acknowledgments

We thank Stephen Barnes and Ray Moore for helpful discussions and technical support, G. Seydoux for the *pie-1* expression plasmid, and the UAB Targeted Metabolomics and Proteomics Laboratory, which has been supported in part by an NCI Core Research Support Grant to the UAB Comprehensive Cancer. We also thank Stephen Barnes, Hugo Bellen, Tika Benveniste, Pauline Cottee, Sung Min Han, Tim Mahoney, and Brad Yoder for comments on the manuscript. Some strains were provided by the *Caenorhabditis* Genetics Center, which is funded by the NIH. The *gst-4* mutant strains were created by the *C. elegans* Gene Knockout Consortium, which is funded by the NIH, and the Japanese National Bioresource Project, which is supported by the Ministry of Education, Culture, Science, Sports and Technology. This work was supported by the NIH (R01GM085105 to MAM, including an ARRA administrative supplement).

References

Burks DJ, Font de Mora J, Schubert M, Withers DJ, Myers MG, Towery HH, Altamuro SL, Flint CL, White MF. IRS-2 pathways integrate female reproduction and energy homeostasis. Nature. 2000; 407:377–382. [PubMed: 11014193]

Burr GO, Burr MM. On the nature and role of the fatty acids essential for nutrition. J Biol Chem. 1930; 86:587–621.

Castrillon DH, Miao L, Kollipara R, Horner JW, DePinho RA. Suppression of ovarian follicle activation in mice by the transcription factor Foxo3a. Science. 2003; 301:215–218. [PubMed: 12855809]

Chandrasekharan NV, Simmons DL. The cyclooxygenases. Genome Biol. 2004; 5:241. [PubMed: 15345041]

Curran SP, Wu X, Riedel CG, Ruvkun G. A soma-to-germline transformation in long-lived Caenorhabditis elegans mutants. Nature. 2009; 459:1079–1084. [PubMed: 19506556]

Daiyasu H, Toh H. Molecular evolution of the myeloperoxidase family. J Mol Evol. 2000; 51:433–445. [PubMed: 11080366]

Dey I, Keller K, Belley A, Chadee K. Identification and characterization of a cyclooxygenase-like enzyme from Entamoeba histolytica. Proc Natl Acad Sci U S A. 2003; 100:13561–13566. [PubMed: 14585927]

Eisenbach M, Giojalas LC. Sperm guidance in mammals - an unpaved road to the egg. Nat Rev Mol Cell Biol. 2006; 7:276–285. [PubMed: 16607290]

Estevez M, Attisano L, Wrana JL, Albert PS, Massague J, Riddle DL. The daf-4 gene encodes a bone morphogenetic protein receptor controlling C. elegans dauer larva development. Nature. 1993; 365:644–649. [PubMed: 8413626]

Evans EA, Chen WC, Tan MW. The DAF-2 insulin-like signaling pathway independently regulates aging and immunity in C. elegans. Aging Cell. 2008; 7:879–893. [PubMed: 18782349]

Fielenbach N, Antebi A. C. elegans dauer formation and the molecular basis of plasticity. Genes Dev. 2008; 22:2149–2165. [PubMed: 18708575]

Funk CD. Prostaglandins and leukotrienes: advances in eicosanoid biology. Science. 2001; 294:1871–1875. [PubMed: 11729303]

Garofalo RS. Genetic analysis of insulin signaling in Drosophila. Trends Endocrinol Metab. 2002; 13:156–162. [PubMed: 11943559]

Gems D, Sutton AJ, Sundermeyer ML, Albert PS, King KV, Edgley ML, Larsen PL, Riddle DL. Two pleiotropic classes of daf-2 mutation affect larval arrest, adult behavior, reproduction and longevity in Caenorhabditis elegans. Genetics. 1998; 150:129–155. [PubMed: 9725835]

Gfeller A, Dubugnon L, Liechti R, Farmer EE. Jasmonate biochemical pathway. Sci Signal. 2010; 3:cm3. [PubMed: 20159849]

Golovko MY, Murphy EJ. An improved LC-MS/MS procedure for brain prostanoid analysis using brain fixation with head-focused microwave irradiation and liquid-liquid extraction. J Lipid Res. 2008; 49:893–902. [PubMed: 18187404]

Grant B, Hirsh D. Receptor-mediated endocytosis in the Caenorhabditis elegans oocyte. Mol Biol Cell. 1999; 10:4311–4326. [PubMed: 10588660]

Gross GA, Imamura T, Luedke C, Vogt SK, Olson LM, Nelson DM, Sadovsky Y, Muglia LJ. Opposing actions of prostaglandins and oxytocin determine the onset of murine labor. Proc Natl Acad Sci U S A. 1998; 95:11875–11879. [PubMed: 9751758]

Halaschek-Wiener J, Khattra JS, McKay S, Pouzyrev A, Stott JM, Yang GS, Holt RA, Jones SJ, Marra MA, Brooks-Wilson AR, Riddle DL. Analysis of long-lived C. elegans daf-2 mutants using serial analysis of gene expression. Genome Res. 2005; 15:603–615. [PubMed: 15837805]

Han SM, Cottee PA, Miller MA. Sperm and oocyte communication mechanisms controlling C. elegans fertility. Dev Dyn. 2010; 239:1265–1281. [PubMed: 20034089]

Henderson ST, Bonafe M, Johnson TE. daf-16 protects the nematode Caenorhabditis elegans during food deprivation. J Gerontol A Biol Sci Med Sci. 2006; 61:444–460. [PubMed: 16720740]

Hertweck M, Gobel C, Baumeister R. C. elegans SGK-1 is the critical component in the Akt/PKB kinase complex to control stress response and life span. Dev Cell. 2004; 6:577–588. [PubMed: 15068796]

Horikawa M, Nomura T, Hashimoto T, Sakamoto K. Elongation and desaturation of fatty acids are critical in growth, lipid metabolism and ontogeny of Caenorhabditis elegans. J Biochem. 2008; 144:149–158. [PubMed: 18424809]

Hughes SE, Evason K, Xiong C, Kornfeld K. Genetic and pharmacological factors that influence reproductive aging in nematodes. PLoS Genet. 2007; 3:e25. [PubMed: 17305431]

Kingsley PJ, Rouzer CA, Saleh S, Marnett LJ. Simultaneous analysis of prostaglandin glyceryl esters and prostaglandins by electrospray tandem mass spectrometry. Anal Biochem. 2005; 343:203–211. [PubMed: 16004953]

Kubagawa HM, Watts JL, Corrigan C, Edmonds JW, Sztul E, Browse J, Miller MA. Oocyte signals derived from polyunsaturated fatty acids control sperm recruitment in vivo. Nat Cell Biol. 2006; 8:1143–1148. [PubMed: 16998478]

Landis JN, Murphy CT. Integration of diverse inputs in the regulation of Caenorhabditis elegans DAF-16/FOXO. Dev Dyn. 2010; 239:1405–1412. [PubMed: 20140911]

Leiers B, Kampkotter A, Grevelding CG, Link CD, Johnson TE, Henkle-Duhrsen K. A stress-responsive glutathione S-transferase confers resistance to oxidative stress in Caenorhabditis elegans. Free Radic Biol Med. 2003; 34:1405–1415. [PubMed: 12757851]

Liang B, Moussaif M, Kuan CJ, Gargus JJ, Sze JY. Serotonin targets the DAF-16/FOXO signaling pathway to modulate stress responses. Cell Metab. 2006; 4:429–440. [PubMed: 17141627]

Lim H, Paria BC, Das SK, Dinchuk JE, Langenbach R, Trzaskos JM, Dey SK. Multiple female reproductive failures in cyclooxygenase 2-deficient mice. Cell. 1997; 91:197–208. [PubMed: 9346237]

Liu L, Rajareddy S, Reddy P, Du C, Jagarlamudi K, Shen Y, Gunnarsson D, Selstam G, Boman K, Liu K. Infertility caused by retardation of follicular development in mice with oocyte-specific expression of Foxo3a. Development. 2007; 134:199–209. [PubMed: 17164425]

Liu Z, Rudd MD, Hernandez-Gonzalez I, Gonzalez-Robayna I, Fan HY, Zeleznik AJ, Richards JS. FSH and FOXO1 regulate genes in the sterol/steroid and lipid biosynthetic pathways in granulosa cells. Mol Endocrinol. 2009; 23:649–661. [PubMed: 19196834]

Luo S, Kleemann GA, Ashraf JM, Shaw WM, Murphy CT. TGF-beta and insulin signaling regulate reproductive aging via oocyte and germline quality maintenance. Cell. 2010; 143:299–312. [PubMed: 20946987]

Masoodi M, Nicolaou A. Lipidomic analysis of twenty-seven prostanoids and isoprostanes by liquid chromatography/electrospray tandem mass spectrometry. Rapid Commun Mass Spectrom. 2006; 20:3023–3029. [PubMed: 16986207]

Matsumoto H, Ma W, Smalley W, Trzaskos J, Breyer RM, Dey SK. Diversification of cyclooxygenase-2-derived prostaglandins in ovulation and implantation. Biol Reprod. 2001; 64:1557–1565. [PubMed: 11319164]

McCarter J, Bartlett B, Dang T, Schedl T. On the control of oocyte meiotic maturation and ovulation in Caenorhabditis elegans. Dev Biol. 1999; 205:111–128. [PubMed: 9882501]

Mendonca LL, Khamashta MA, Nelson-Piercy C, Hunt BJ, Hughes GR. Non-steroidal anti-inflammatory drugs as a possible cause for reversible infertility. Rheumatology (Oxford). 2000; 39:880–882. [PubMed: 10952743]

Miller MA, Cutter AD, Yamamoto I, Ward S, Greenstein D. Clustered organization of reproductive genes in the C. elegans genome. Curr Biol. 2004; 14:1284–1290. [PubMed: 15268860]

Miller MA, Nguyen VQ, Lee MH, Kosinski M, Schedl T, Caprioli RM, Greenstein D. A sperm cytoskeletal protein that signals oocyte meiotic maturation and ovulation. Science. 2001; 291:2144–2147. [PubMed: 11251118]

Mukhopadhyay A, Oh SW, Tissenbaum HA. Worming pathways to and from DAF-16/FOXO. Exp Gerontol. 2006; 41:928–934. [PubMed: 16839734]

Murphy CT, McCarroll SA, Bargmann CI, Fraser A, Kamath RS, Ahringer J, Li H, Kenyon C. Genes that act downstream of DAF-16 to influence the lifespan of Caenorhabditis elegans. Nature. 2003; 424:277–283. [PubMed: 12845331]

Murphy RC, Barkley RM, Zemski Berry K, Hankin J, Harrison K, Johnson C, Krank J, McAnoy A, Uhlson C, Zarini S. Electrospray ionization and tandem mass spectrometry of eicosanoids. Anal Biochem. 2005; 346:1–42. [PubMed: 15961057]

Ogg S, Paradis S, Gottlieb S, Patterson GI, Lee L, Tissenbaum HA, Ruvkun G. The Fork head transcription factor DAF-16 transduces insulin-like metabolic and longevity signals in C. elegans. Nature. 1997; 389:994–999. [PubMed: 9353126]

Oh SW, Mukhopadhyay A, Dixit BL, Raha T, Green MR, Tissenbaum HA. Identification of direct DAF-16 targets controlling longevity, metabolism and diapause by chromatin immunoprecipitation. Nat Genet. 2006; 38:251–257. [PubMed: 16380712]

Pall M, Friden BE, Brannstrom M. Induction of delayed follicular rupture in the human by the selective COX-2 inhibitor rofecoxib: a randomized double-blind study. Hum Reprod. 2001; 16:1323–1328. [PubMed: 11425807]

Pisarska MD, Kuo FT, Tang D, Zarrini P, Khan S, Ketefian A. Expression of forkhead transcription factors in human granulosa cells. Fertil Steril. 2009; 91:1392–1394. [PubMed: 18692812]

Praitis V, Casey E, Collar D, Austin J. Creation of low-copy integrated transgenic lines in Caenorhabditis elegans. Genetics. 2001; 157:1217–1226. [PubMed: 11238406]

Reinke V, Gil IS, Ward S, Kazmer K. Genome-wide germline-enriched and sex-biased expression profiles in Caenorhabditis elegans. Development. 2004; 131:311–323. [PubMed: 14668411]

Rowley AF, Vogan CL, Taylor GW, Clare AS. Prostaglandins in non-insectan invertebrates: recent insights and unsolved problems. J Exp Biol. 2005; 208:3–14. [PubMed: 15601872]

Schackwitz WS, Inoue T, Thomas JH. Chemosensory neurons function in parallel to mediate a pheromone response in C. elegans. Neuron. 1996; 17:719–728. [PubMed: 8893028]

Shapira M, Hamlin BJ, Rong J, Chen K, Ronen M, Tan MW. A conserved role for a GATA transcription factor in regulating epithelial innate immune responses. Proc Natl Acad Sci U S A. 2006; 103:14086–14091. [PubMed: 16968778]

Shaw WM, Luo S, Landis J, Ashraf J, Murphy CT. The C. elegans TGF-beta Dauer pathway regulates longevity via insulin signaling. Curr Biol. 2007; 17:1635–1645. [PubMed: 17900898]

Sirois J, Sayasith K, Brown KA, Stock AE, Bouchard N, Dore M. Cyclooxygenase-2 and its role in ovulation: a 2004 account. Hum Reprod Update. 2004; 10:373–385. [PubMed: 15205395]

Smith G, Roberts R, Hall C, Nuki G. Reversible ovulatory failure associated with the development of luteinized unruptured follicles in women with inflammatory arthritis taking non-steroidal anti-inflammatory drugs. Br J Rheumatol. 1996; 35:458–462. [PubMed: 8646437]

Smith LH, Petrie MS, Morrow JD, Oates JA, Vaughan DE. The sterol response element binding protein regulates cyclooxygenase-2 gene expression in endothelial cells. J Lipid Res. 2005; 46:862–871. [PubMed: 15716578]

Sommer A, Rickert R, Fischer P, Steinhart H, Walter RD, Liebau E. A dominant role for extracellular glutathione S-transferase from Onchocerca volvulus is the production of prostaglandin D2. Infect Immun. 2003; 71:3603–3606. [PubMed: 12761146]

Stanley-Samuelson DW, Pedibhotla VK. What can we learn from prostaglandins and related eicosanoids in insects? Insect Biochem Mol Biol. 1996; 26:223–234. [PubMed: 8900594]

Sze JY, Victor M, Loer C, Shi Y, Ruvkun G. Food and metabolic signalling defects in a Caenorhabditis elegans serotonin-synthesis mutant. Nature. 2000; 403:560–564. [PubMed: 10676966]

Tatar M, Bartke A, Antebi A. The endocrine regulation of aging by insulin-like signals. Science. 2003; 299:1346–1351. [PubMed: 12610294]

Tissenbaum HA, Ruvkun G. An insulin-like signaling pathway affects both longevity and reproduction in Caenorhabditis elegans. Genetics. 1998; 148:703–717. [PubMed: 9504918]

Tootle TL, Spradling AC. Drosophila Pxt: a cyclooxygenase-like facilitator of follicle maturation. Development. 2008; 135:839–847. [PubMed: 18216169]

Troemel ER, Chu SW, Reinke V, Lee SS, Ausubel FM, Kim DH. p38 MAPK regulates expression of immune response genes and contributes to longevity in C. elegans. PLoS Genet. 2006; 2:e183. [PubMed: 17096597]

Vane JR. Inhibition of prostaglandin synthesis as a mechanism of action for aspirin-like drugs. Nat New Biol. 1971; 231:232–235. [PubMed: 5284360]

Watts JL, Browse J. Genetic dissection of polyunsaturated fatty acid synthesis in Caenorhabditis elegans. Proc Natl Acad Sci U S A. 2002; 99:5854–5859. [PubMed: 11972048]

Watts JL, Phillips E, Griffing KR, Browse J. Deficiencies in C20 polyunsaturated fatty acids cause behavioral and developmental defects in Caenorhabditis elegans fat-3 mutants. Genetics. 2003; 163:581–589. [PubMed: 12618397]

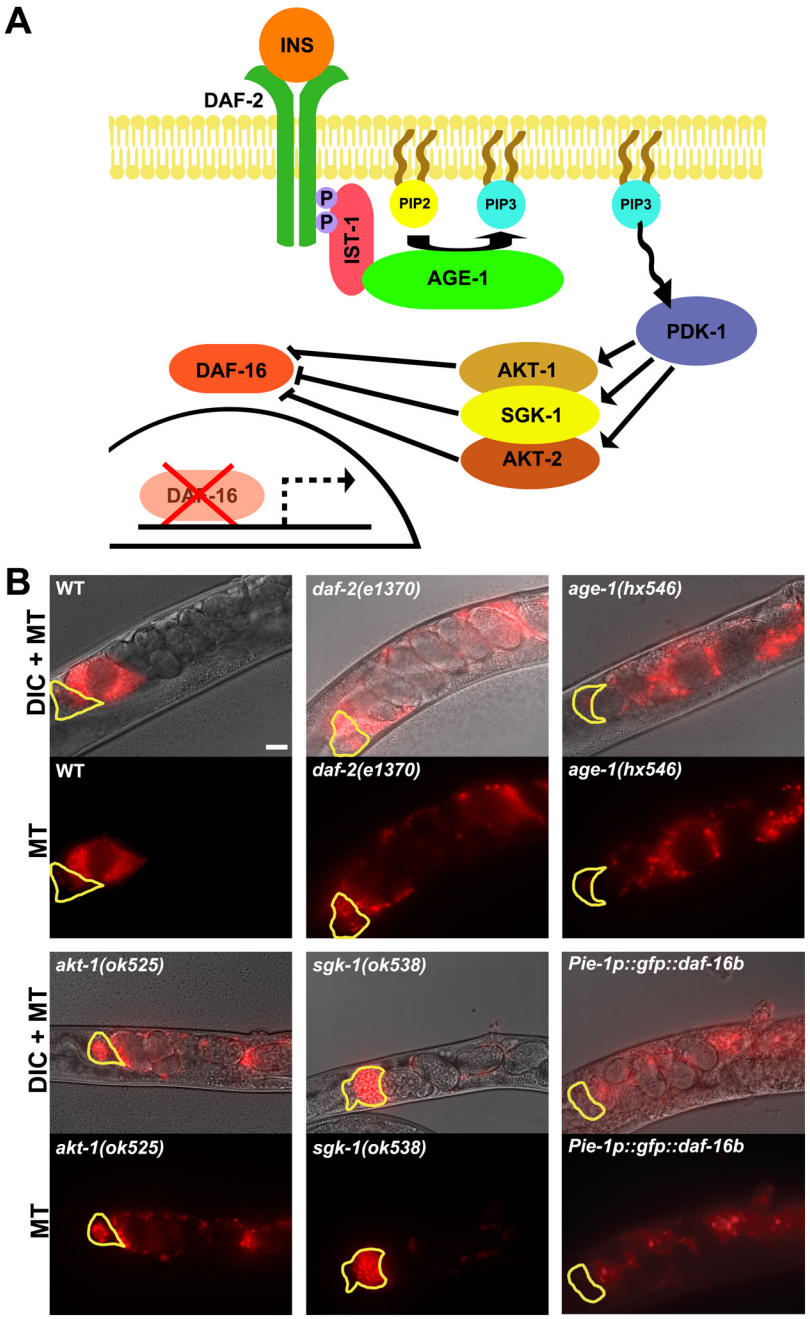

Figure 1. Insulin signaling is required cell nonautonomously for sperm guidance

(A) Canonical insulin signaling pathway in *C. elegans*.

(B) Representative sperm distribution images 1 hour after mating wild-type or mutant hermaphrodites to wild-type MitoTracker-labelled (MT) males. Quantification of selected genotypes is shown in Fig. 2. Yellow outline marks the spermatheca. Vulva is to the right (see Fig. 2A for gonad diagram). Bar, 20 μm.

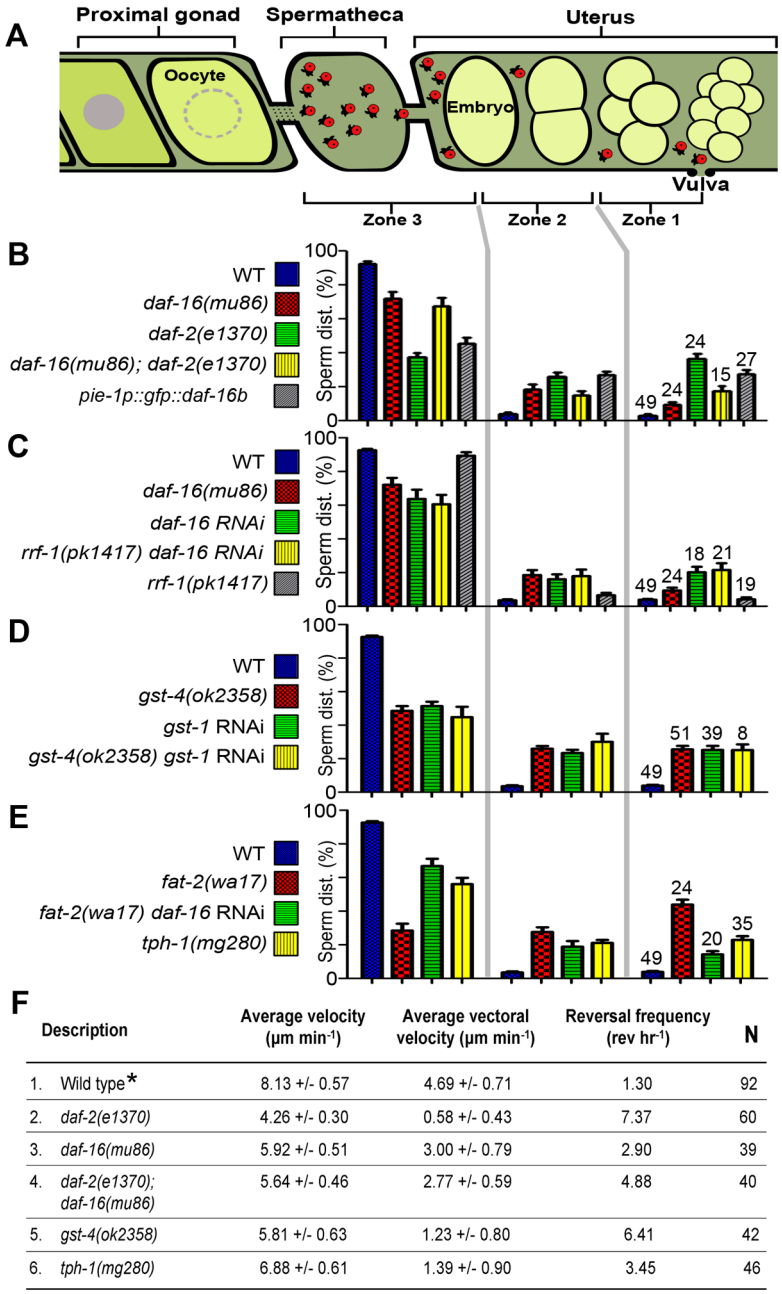

F

Description	Average velocity (μm min^{-1})	Average vectoral velocity (μm min^{-1})	Reversal frequency (rev hr^{-1})	N
1. Wild type*	8.13 +/- 0.57	4.69 +/- 0.71	1.30	92
2. *daf-2(e1370)*	4.26 +/- 0.30	0.58 +/- 0.43	7.37	60
3. *daf-16(mu86)*	5.92 +/- 0.51	3.00 +/- 0.79	2.90	39
4. *daf-2(e1370); daf-16(mu86)*	5.64 +/- 0.46	2.77 +/- 0.59	4.88	40
5. *gst-4(ok2358)*	5.81 +/- 0.63	1.23 +/- 0.80	6.41	42
6. *tph-1(mg280)*	6.88 +/- 0.61	1.39 +/- 0.90	3.45	46

Figure 2. Quantification of sperm guidance defects

(A) Sperm guidance is evaluated by mating MT-labelled males to hermaphrodites and measuring accumulation at the spermatheca 1 hour after mating, as well as migration velocity, directional velocity, and reversal frequency in the uterus (Kubagawa et al., 2006). **(B-E)** Sperm distribution 1 hour after mating. Equal distribution in each zone is consistent with random sperm motility. The number of gonads analyzed is shown above the zone 1 distributions. Error bars are SEM. See supplemental experimental procedures for zone definitions. Feeding RNAi was initiated at the L4 or young adult stages.

(F) Sperm motility values in wild-type and mutant hermaphrodite uteri are measured from time-lapse videos after mating. Vectoral velocity is directional velocity toward the spermatheca. N indicates number of sperm analyzed. *, Wild-type sperm values include new

data (N = 18) and published data (Kubagawa et al., 2006). Values +/− SEM are shown. *P* values were calculated using a Student T-test.

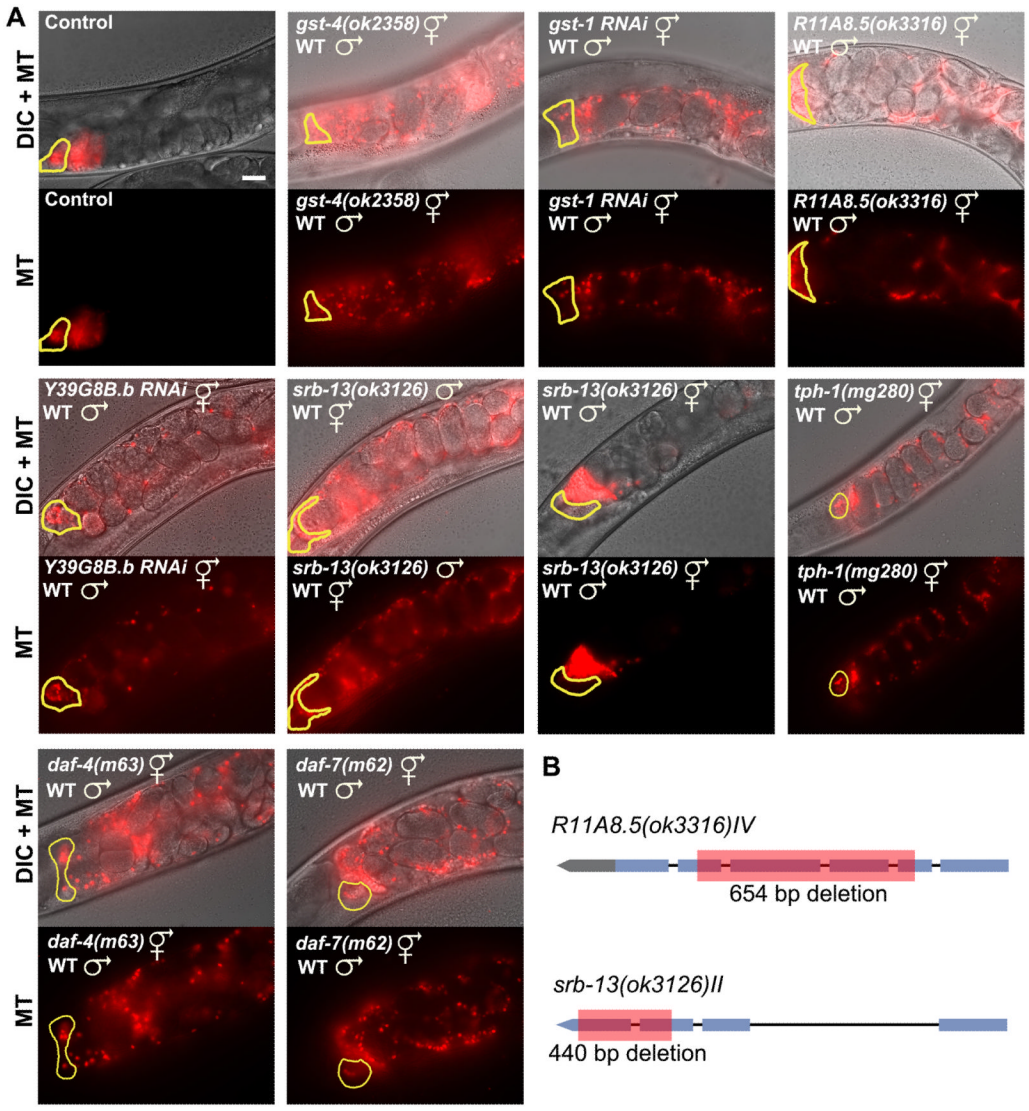

Figure 3. Representative sperm distribution images

(A) Representative sperm distribution images 1 hour after mating wild-type or mutant hermaphrodites to wild-type or mutant MT males. All predicted PG synthase mutant and RNAi hermaphrodites have variable nonautonomous defects, with *R11A8.5* mutants having the weakest phenotype (more severe case is shown). *C35D10.6* RNAi (not shown) is similar to *Y39G8B.2* RNAi (shown). Quantification of selected genotypes is shown in Fig. 2. Yellow outline marks the spermatheca. Vulva is to the right (see Fig. 2A for gonad diagram). Bar, 20 μm.

(B) Predicted gene structures and deletions. The *ok2358* mutation deletes all four *gst-4* exons (not shown).

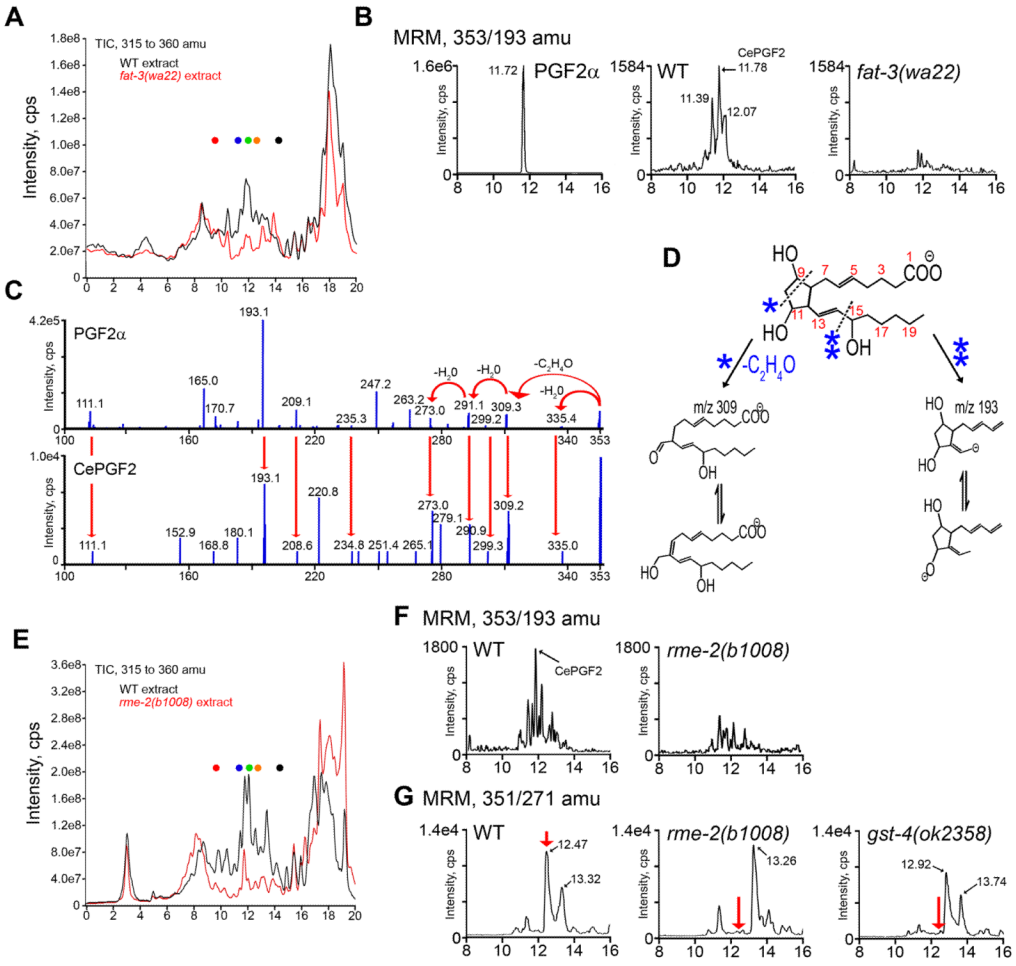

Figure 4. *C. elegans* oocytes synthesize F-series PGs

(A) TICs for *m/z* 315–360 of wild-type (WT, black) and *fat-3(wa22)* extracts (red). Each peak contains numerous ions. Dots represent retention times for 20-OH PGE_2 (red), $PGF_{3\alpha}$ (blue), $PGF_{2\alpha}$(green), PGD_2 (orange), and PGB_2 (black) standards (see Supplemental Table S2).

(B) MRM chromatograms using the mass transition *m/z* 353/193 of $PGF_{2\alpha}$ wild-type extracts, and *fat-3(wa22)* mutant extracts.

(C) LC-MS/MS of *m/z* 353, $[M\text{-}H]^-$ of authentic $PGF_{2\alpha}$ (top) and CePGF2 (bottom).

(D) Authentic $PGF_{2\alpha}$ fragmentation patterns showing predicted structures (*m/z* 309 and *m/z* 193) that are characteristic of F-series PGs.

(E) TICs for *m/z* 315–360 of wild-type (black) and *rme-2(b1008)* extracts (red).

(F) MRM chromatograms using the mass transition *m/z* 353/193 of wild-type and *rme-2* mutant extracts.

(G) MRM chromatograms using the mass transition *m/z* 351/271 of wild-type extracts, *rme-2(b1008)*, and *gst-4(ok2358)* mutant extracts. The major peak (arrow) in wild-type hermaphrodites from Rt~12.3–12.9 contains a mixture of ions that are dependent on *rme-2* and *gst-4* function. LC-MS/MS indicates the ion at Rt=12.5 (Supplemental Fig. S2, top) is an unsaturated $PGF_{2\alpha}$ analog. Notice that ions at 12.92 and 13.74 are the most abundant in *gst-4* mutants, contrasting with WT and *rme-2* mutants.

Retention times (Rts) in panels A, B, E, F, and G are shown on the X-axis. Identical tissue amounts, extraction conditions, and LC-MS/MS conditions were used for all direct

comparisons. TICs in panels A and E are from independent experiments with different tissue amounts (4.2g for A vs. 6.6g for E) and solvent batches. TIC, total ion chromatogram; MRM, multiple reaction monitoring. TICs show global views of lipid levels (ions between 315 and 360 amu), whereas MRM detects and quantifies individual ions.

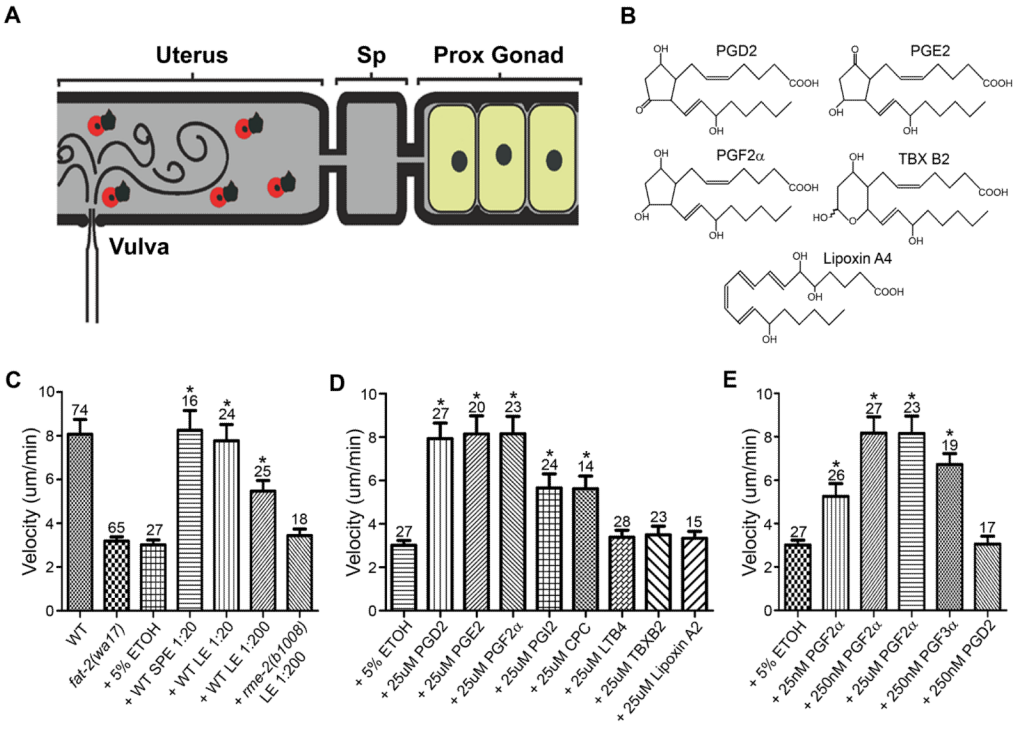

Figure 5. F-series PGs stimulate sperm motility *in vivo*

(A) Diagram showing the microinjection method (see Methods). Sperm motility is assessed within minutes following injection. Wild-type sperm migrate slower in PUFA-deficient *fat-2(wa17)* and *rme-2(b1008)* hermaphrodite uteri compared to wild-type uteri, ~3.1 microns/min versus 8.1 microns/min (Kubagawa et al., 2006).

(B) Structures of selected microinjected eicosanoids.

(C-E) Sperm velocity data following microinjection of extracts (C) or eicosanoids (D, E) through the vulva into *fat-2(wa17)* mutant uteri. Solid phase extraction (SPE) and liquid/liquid extraction (LE) of wild-type hermaphrodites produced identical results, although LE was the preferred method. Similar results are observed when microinjecting into *rme-2(b1008)* mutants (data not shown). Data are from 3 to 10 microinjections per experiment. The major structural difference between inactive Thromboxane B_2 (TBX B2) and active $PGF_{2\alpha}$ is an oxygen that interrupts the cyclopentane ring. *, $P < 0.001$ compared to the 5% ethanol control by a Student T-test. Error bars are SEM. Number of sperm analyzed is above the error bars. Sp, spermatheca; Prox, proximal; ETOH, ethanol; CPC, Carbaprostacyclin; LTB4, Leukotriene B4.

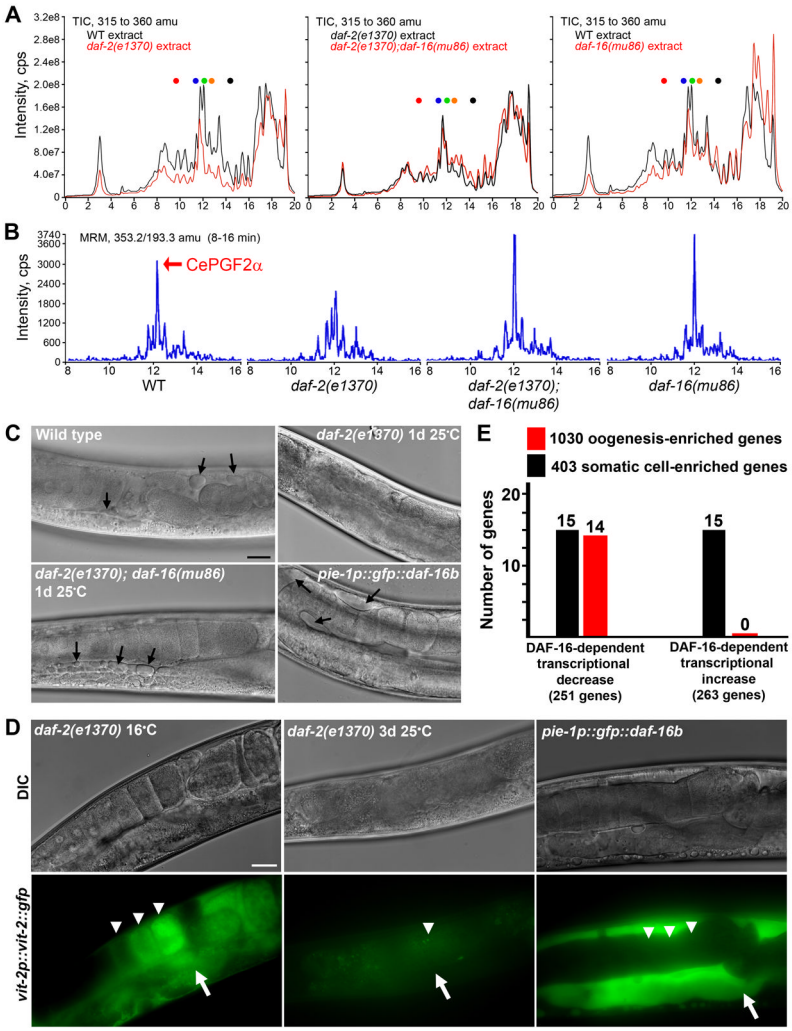

Figure 6. Insulin/FOXO signaling regulates oocyte PG synthesis

(A) TICs for *m/z* 315–360 of wild-type and mutant extracts. Retention times are on the X-axis. Dots represent retention times of PG standards described in Fig. 4.

(B) MRM chromatograms using the mass transition *m/z* 353/193 comparing wild-type to mutant extracts.

(C) DIC micrographs of proximal gonads. Yolk (arrows) can be observed in pools within the pseudocoelom and gonad.

(D) *vit-2p::vit-2::gfp* transgene expression. *vit-2::gfp* is incorporated into yolk in the intestine (arrows) and secreted yolk is endocytosed into oocytes (arrowheads). VIT-2::GFP is much brighter than GFP::DAF-16B, which is not visible in the panel. The most proximal oocytes are to the right.

(E) DNA microarray data showing DAF-16-regulating genes expressed in the adult germ line undergoing oogenesis and in somatic cells. Bars in C and D, 20 μm.

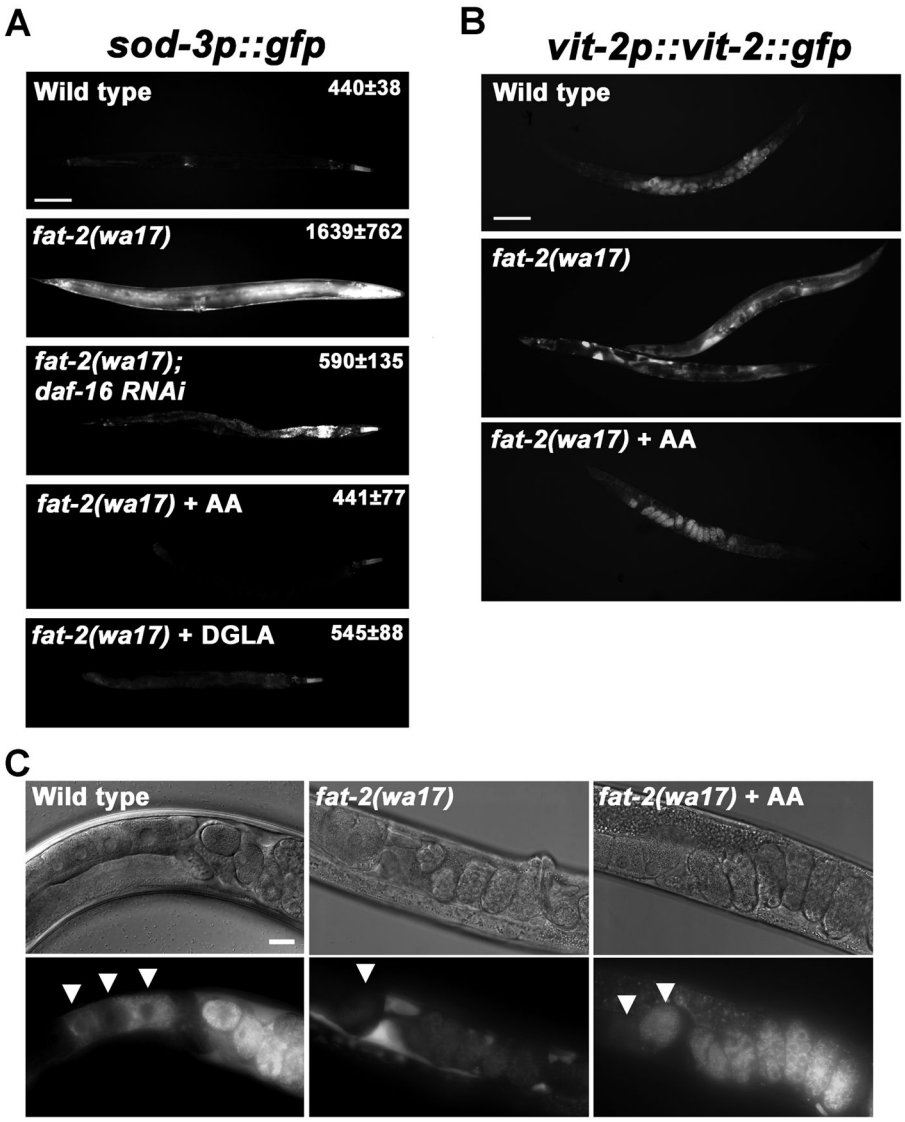

Figure 7. PUFAs inhibit DAF-16/FOXO transcriptional activity and promote yolk endocytosis

(A) Transgenic strains expressing GFP (shown in white) under control of the *sod-3* promoter, a direct DAF-16 target. Numbers indicate average fluorescent intensity ± standard deviation for selected regions adjacent to the intestine (N > 10 animals). *daf-16* RNAi and *fat-2(wa17)* control RNAi (not shown) animals have increased intestinal autofluorescence, easily distinguished from GFP at high magnification, caused by the HT115 feeding RNAi bacterial strain. Anterior is to the right. Bar, 100 μm.

(B) VIT-2::GFP localization driven by the integrated *vit-2p::vit-2::gfp* transgene. Yolk pools are observed in *fat-2(wa17)* mutants. Bar, 100 μm.

(C) High magnification images showing VIT-2::GFP endocytosis into oocytes (arrowheads). Bar, 20 μm. AA, Arachidonic acid; DGLA, Dihomo-gamma-linolenic acid.

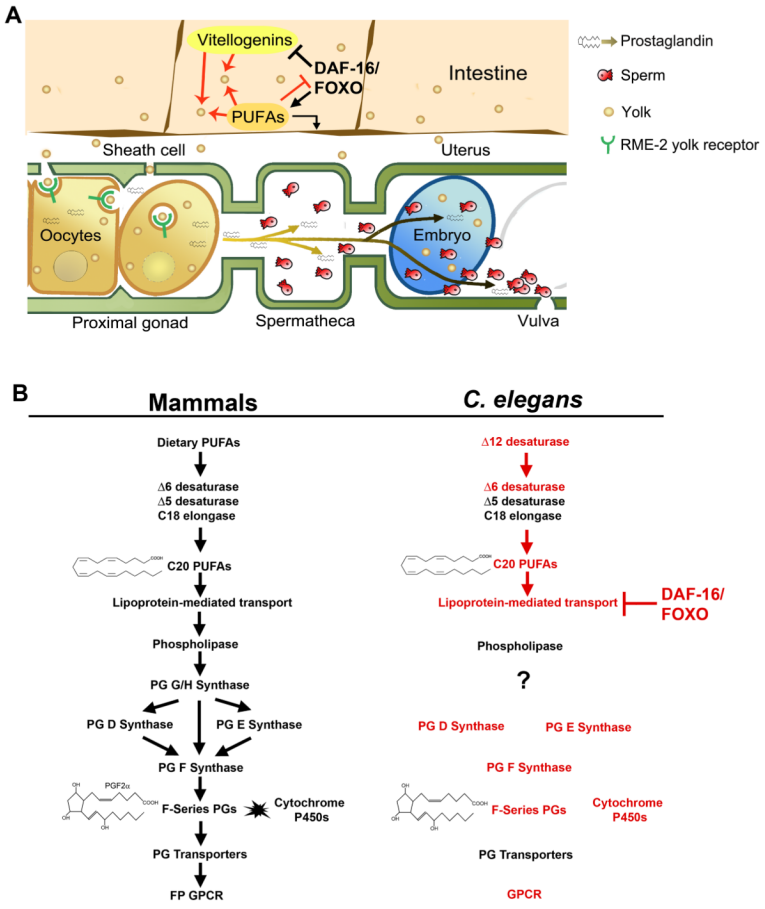

Figure 8. Working models

(A) Cell type and molecular regulation. DAF-16 promotes intestinal PUFA biosynthesis through increased expression of *fat* genes and inhibits yolk lipoprotein complex formation required to transport PUFAs to oocytes. Increased DAF-16 activity shifts the PG balance, favoring those PGs requiring *de novo* PUFA synthesis over those requiring PUFA transport to distant sites. Yolk provides oocytes with PUFAs for synthesizing F-series PGs that promote sperm guidance. PUFAs negatively regulate DAF-16 to promote oocyte yolk endocytosis and PG synthesis. See text for additional details.

(B) Prostaglandin synthesis machinery in mammals and predicted *C. elegans* pathway. The *C. elegans* genome encodes homologs of mammalian enzymes that synthesize and modify PGs, with the lone exception being PG G/H synthase. Red color indicates steps required for sperm guidance, based on genetic or biochemical studies (this study and Kubagawa et al., 2006). Red arrows indicate biochemically conserved steps. See text for additional details.